Published online 22 August 2018

Nucleic Acids Research, 2018, Vol. 46, No. 18 ***9537–9549***
doi: 10.1093/nar/gky764

Base and nucleotide excision repair facilitate resolution of platinum drugs-induced transcription blockage

Jana Slyskova[1], Mariangela Sabatella[1], Cristina Ribeiro-Silva[1,2], Colin Stok[1], Arjan F. Theil[1,2], Wim Vermeulen[1,2] and Hannes Lans[1,2,*]

[1]Department of Molecular Genetics, Erasmus MC, Erasmus University Medical Center Rotterdam, 3000 CA Rotterdam, The Netherlands and [2]Oncode Institute, Erasmus MC, Erasmus University Medical Center Rotterdam, 3000 CA Rotterdam, The Netherlands

Received June 14, 2018; Revised August 08, 2018; Editorial Decision August 10, 2018; Accepted August 20, 2018

ABSTRACT

Sensitivity and resistance of cells to platinum drug chemotherapy are to a large extent determined by activity of the DNA damage response (DDR). Combining chemotherapy with inhibition of specific DDR pathways could therefore improve treatment efficacy. Multiple DDR pathways have been implicated in removal of platinum-DNA lesions, but it is unclear which exact pathways are most important to cellular platinum drug resistance. Here, we used CRISPR/Cas9 screening to identify DDR proteins that protect colorectal cancer cells against the clinically applied platinum drug oxaliplatin. We find that besides the expected homologous recombination, Fanconi anemia and translesion synthesis pathways, in particular also transcription-coupled nucleotide excision repair (TC-NER) and base excision repair (BER) protect against platinum-induced cytotoxicity. Both repair pathways are required to overcome oxaliplatin- and cisplatin-induced transcription arrest. In addition to the generation of DNA crosslinks, exposure to platinum drugs leads to reactive oxygen species production that induces oxidative DNA lesions, explaining the requirement for BER. Our findings highlight the importance of transcriptional integrity in cells exposed to platinum drugs and suggest that both TC-NER and BER should be considered as targets for novel combinatorial treatment strategies.

INTRODUCTION

Platinum-based chemotherapy is among the most widely used treatments of solid tumors (1,2). Its anti-cancer potency is due to formation of platinum-DNA adducts, mainly between adjacent purines generating intrastrand crosslinks (80–90%), or between bases on opposite strands giving rise to interstrand crosslinks (ICLs). Cytotoxicity of these DNA lesions is thought to be derived from impediment of transcription and replication, which eventually causes cell cycle arrest or apoptosis (3). Three platinum drugs are currently widely approved for cancer treatment in humans: cisplatin, carboplatin and oxaliplatin. Platinum chemotherapy responses vary greatly among different tumor types. Oxaliplatin is exclusively used to treat colon and rectal cancer, against which the other two drugs lack therapeutic efficacy (1). This drug specificity is, however, poorly understood. Genetic variability in drug transport, metabolism and cellular defense systems such as the DNA damage response (DDR), likely account for differences in tumor sensitivity. The importance of the DDR is exemplified by testicular carcinoma of which the sensitivity to cisplatin correlates with protein levels of specific DNA repair proteins (4,5).

Cells utilize several DDR pathways to cope with DNA damage. The choice of the pathway depends on the cell cycle stage, the type of DNA lesion and its genomic location (6,7). For instance, small nucleobase modifications are repaired by base excision repair (BER), initiated by lesion-specific DNA glycosylases that recognize and remove damaged bases (8,9). Cleavage of the sugar-phosphate backbone by APE1 is followed by PARP1-dependent DNA synthesis and ligation, involving the BER-specific polymerase beta (POLB) and the DNA ligase III-XRCC1 complex. Helix-distorting lesions, such as UV photoproducts and intrastrand crosslinks, are repaired by nucleotide excision repair (NER) (10,11). NER is initiated by two DNA damage

*To whom correspondence should be addressed. Tel: +31 10 7038169; Fax: +31 10 7044743; Email: w.lans@erasmusmc.nl
Present address: Colin Stok, Department of Medical Oncology, University Medical Center Groningen, University of Groningen, 9713 GZ Groningen, The Netherlands.

recognition subpathways: transcription-coupled NER (TC-NER) and global-genome NER (GG-NER). In TC-NER, damage is detected by lesion-stalling of RNA polymerase 2 (RNAP2), which triggers recruitment of the UVSSA, CSB and CSA proteins that are essential for the assembly of downstream NER factors. In GG-NER, lesions are detected anywhere in the genome by the coordinated activity of the UV-DDB and XPC/RAD23B/CETN2 complexes. Both damage detection mechanisms utilize the same machinery to excise the damaged strand by means of the ERCC1/XPF and XPG endonucleases. The resulting gap is then filled in by DNA synthesis and ligation. Double-strand breaks (DSBs) can be resolved by different repair pathways, mainly depending on the type of break and cell cycle phase. Non-homologous end-joining (NHEJ) re-ligates broken DNA ends in any cell cycle phase, while homologous recombination (HR) acts only in S/G2 phase and employs the sister chromatid as repair template (12). Finally, removal of more complex lesions like ICLs requires the collaborative effort of multiple DDR pathways. Cell cycle phase dictates the choice of the particular repair response, but the mechanisms are still only partially understood. Briefly, stalling of a replication fork on an ICL leads to lesion recognition by the Fanconi anemia (FA) pathway and unhooking of the ICL by DNA incision, generating a DSB (13). ERCC1/XPF is thought to be the main endonuclease responsible for ICL unhooking, but other nucleases are likely also involved (14,15). Translesion synthesis (TLS) fills the gap opposite of the unhooked crosslink, to generate an intact template for the HR pathway, which repairs the DSB. The unhooked crosslink is probably repaired by NER. Both NER and TLS are also implicated in removal of ICLs in non-replicating cells but the mechanism involved is even less well understood (16,17).

DNA lesions induced by platinum drugs were suggested to trigger the response of multiple repair mechanisms (2,3). Given the importance of DDR in removal of platinum-DNA adducts, much effort has also been put into linking variations in DNA repair capacity and DDR gene expression and polymorphisms to platinum drug responses, with varying success (18). Still, it remains unclear which DDR pathways are most important in determining cancer cell sensitivity or resistance. Therefore, we applied CRISPR-based genetic screening to identify DDR genes that sensitize colon cancer cells to platinum drugs. We show that oxaliplatin and cisplatin strongly inhibit transcription and that, besides FA, TLS and HR, also TC-NER and BER are essential to protect cancer cells against platinum drug cytotoxicity by resolving platinum drug-induced transcription blockage.

MATERIALS AND METHODS

Cell culture

Colon adenocarcinoma cells DLD-1 (Horizon Discovery) were cultured in a 1:1 mixture of Roswell Park Memorial Institute-1640 medium (Sigma-Aldrich) and Ham's F-10 nutrient mix (Lonza), supplemented with 10% fetal calf serum (FCS; BioWest), and 1% penicillin/streptomycin (Sigma-Aldrich). Human embryonic kidney cells HEK-293T, osteosarcoma cells U2OS, hTERT-immortalized human fibroblasts VH10, SV40-transformed human fibroblasts C5RO, XP4PA (XPC-deficient) (19), CS1AN (CSB-deficient) (20), CS1AN complemented with YFP-CSB^{del} (21), and XRCC1-YFP expressing MRC-5 were cultured in a 1:1 mixture of Dulbecco's Modified Eagle medium (Lonza) and Ham's F-10, supplemented with 10% FCS, 1% penicillin/streptomycin, 2 mM UltraGlutamine (Lonza), and 0.1 mM MEM Eagle non-essential amino acid solution (Lonza). All cells were cultured at 37°C, in 20% O_2 and 5% CO_2, except for VH10 cells that were cultured at 3% O_2. To generate MRC-5 cells expressing XRCC1-YFP, XRCC1-YFP cDNA (a gift from Anna Campalans) (22) was cloned into pLenti-CMV-Puro-DEST (a gift from Eric Campeau & Paul Kaufman) (23). Following lentiviral transduction, MRC-5 cells stably expressing XRCC1-YFP were selected by puromycin and fluorescence-activated cell sorting.

Chemicals

Oxaliplatin and cisplatin (Sigma-Aldrich) were dissolved in PBS, aliquoted and stored at -20°C. Treatment concentration and duration are indicated for each experiment. 8-methoxypsoralen (8-MOP, Sigma-Aldrich) dissolved in DMSO was used in 50 μM concentration for 2 h. To inhibit PARP, cells were treated for 24 h with 10 μM olaparib dissolved in PBS (Selleckchem). To inhibit POLB, cells were treated for 24 h with 500 μM pamoic acid (Sigma-Aldrich) dissolved in 200 mM NaCl and 20 mM Tris–HCl. To inhibit transcription, cells were treated for 1 h with 1 μM flavopiridol (Sigma-Aldrich), dissolved in DMSO. Trolox (Sigma-Aldrich) was dissolved in ethanol and applied for 24 h prior to an experiment at a concentration of 600 μM.

Generation of knockout cell lines

For genetic screening (Figure 1), 85 populations of DLD-1 cells, each expressing a unique sgRNA targeting one out of 43 DNA repair genes (Supplementary Table S1), were generated by lentiviral transduction. For each gene, two different sgRNAs complementary to an early exon were designed (except for *XPA* which was targeted by one sgRNA only) using the CRISPR Design Tool (http://crispr.mit.edu/) (24). Each separate sgRNA was cloned into plentiCRISPRv2 (a gift from Feng Zhang) (25), which was transfected into HEK-293T cells using jetPEI® (Polyplus Transfection), together with pMDLg/pRRE, pRSV-Rev and pMD2.G (gifts from Didier Trono) (26), to generate lentiviruses. Lentiviral particles were harvested 48 h after transfection and used to transduce DLD-1 cells for 24 h, after which transduced cells were selected with puromycin. Survival experiments with transduced heterogeneous cell populations were performed within four weeks after transduction. To generate stable knockout (KO) DLD-1 cell lines, cells were transiently transfected with plentiCRISPRv2 carrying sgRNAs targeting *CSA*, *XPF*, *POLB*, *PARP1, XRCC1* (Supplementary Table S1) and *CSB* (5′-GCGAGGGCTGAACGGGATGG-3′ and 5′-TGGGTGTTACAGTCAGCACC-3′). Transfected cells were selected by puromycin, clonally expanded and KO was verified by immunoblot.

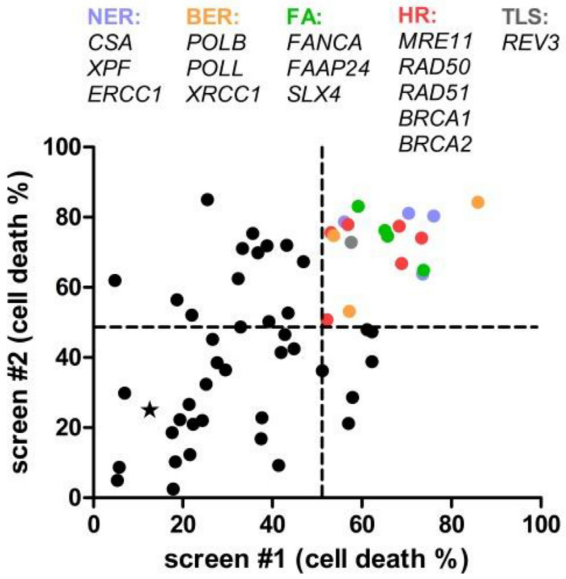

Figure 1. Oxaliplatin sensitivity of DLD-1 cells with CRISPR-induced loss-of-function mutations in DNA repair genes. Each dot represents a cell line stably expressing a unique sgRNA targeting a DNA repair gene as listed in Supplementary Table S1. Responses to an IC_{20} concentration of oxaliplatin (15 μM) of all cell lines were evaluated by MTT assay in two independent screens and expressed as percentage cell death of treated versus untreated cells. Top candidate genes are represented by distinct colors corresponding to their main involvement in different DNA repair pathways (nucleotide and base excision repair, NER and BER; Fanconi anemia, FA; homologous recombination, HR; translesion synthesis, TLS). Most top hits were identified by one of two sgRNAs, except *XPF*, *FANCA* and *RAD51,* which are represented by both sgRNAs. Wild type cells are indicated by the star.

siRNA transfection

siRNA transfections were performed using RNAiMax (Invitrogen) 2 days before each experiment, according to the manufacturer's instructions. siRNA oligomers were purchased from GE healthcare: CTRL (D-001210-05), OGG1 (L-005147-00), and XPA (5′-CUGAUGAUAAACACAAGCUUAUU-3′).

Tracking of indels by decomposition

Tracking of indels by decomposition (TIDE) (27) was used to analyze insertion/deletion (indel) frequency in DLD-1 cells transduced with sgRNA lentiviruses. Genomic DNA was isolated using PureLink® Genomic DNA Mini Kit (Invitrogen) and a 601–840 base pair fragment spanning each sgRNA target site was amplified by PCR using primers listed in Supplementary Table S2. PCR amplicons were isolated from gel and sequenced to determine indel frequency using the TIDE web tool (https://tide.nki.nl/).

Cell viability assays

Cellular response to oxaliplatin and cisplatin was measured by MTT CellTiter 96® non-radioactive cell proliferation assay (Promega). Cells were seeded at a density of 2500 cells per well in 96-well plates in triplicate and grown to ∼20% confluency. Oxaliplatin or cisplatin were added into the medium at 20% of inhibitory concentration (IC_{20}), which was determined from dose-response curves applying non-linear regression (Graph Prism, data not shown). IC_{20} concentration for wild type (WT) DLD-1 cells corresponded to 15 μM of oxaliplatin and 10 μM of cisplatin. After 3 days of treatment, residual cell viability was measured by addition of MTT solution following the manufacturer's recommendations. Absorbance at 490 nm was measured using GloMax®-Multi Detection System (Promega). For clonogenic survival assays, 400 cells per well were seeded in 6-well plates in triplicate. The next day, cells were irradiated with UV-C (254 nm; TUV lamp, Phillips) or treated with oxaliplatin for 24 h, at the indicated dose. Cells were fixed with 50% methanol, 14% acetic acid, and 0.2% Coomassie Brilliant Blue (Sigma-Aldrich) 7 days later. Colonies were counted with colony counter GelCount (Oxford Optronics).

Immunoblotting

Cells were lysed in sample buffer (125 mM Tris–HCl pH 6.8, 20% Glycerol, 10% 2-β-mercaptoethanol, 4% SDS, 0.01% Bromophenol Blue) and boiled for 5 min at 98°C. Proteins were separated in SDS-PAGE gels and transferred onto PVDF membranes (0.45 μm, Merck Millipore). After 1 h of blocking in 5% BSA in PBS-T (0.05% Tween 20), membranes were incubated with primary antibodies in PBS-T at 4°C overnight. Antibodies were against CSA (EPR9237, 1:1000, Abcam, ab137033), CSB (E-18, 1:250, Santa Cruz, sc-10459), XPF (3F2/3, 1:500, Santa Cruz, sc-136153), XPA (FL-273, 1:250, Santa Cruz, sc-853), POLB (1:2000, Abcam, ab26343), PARP1 (F1-23, 1:1000, Alexis Biochemicals, ALX-804-211), XRCC1 (C-15, 1:500, Santa Cruz, sc-5903), OGG1 (EPR4664(2), 1:1000, Abcam, ab124741) and, as loading control, against Ku70 (M-19, 1:1000, Santa Cruz, sc-1487), Tubulin (B-512, 1:5000, Sigma-Aldrich, T6074) and Aquarius (1:1000, Bethyl Laboratories, A302-547A). Anti-mouse, anti-goat and anti-rabbit secondary antibodies, conjugated to CF™680 or CF™770 dyes (Sigma-Aldrich) were used at a dilution of 1:10 000. Probed membranes were visualized with the Odyssey CLx Infrared Imaging System (LI-COR Biosciences).

Psoralen crosslinks induction and immunofluorescence

To generate localized psoralen-induced intrastrand crosslinks and ICLs, U2OS and YFP-CSB^{del} expressing CS1AN cells were grown on 24 mm coverslips and treated with 50 μM of 8-MOP for 2 h. A 355-nm UV-A laser, set at 24% intensity laser power and low (8%) speed, attached to a PALM laser dissection microscope (Zeiss) equipped with a 40× 0.60 NA Korr LD Plan Neofluar objective, was used to activate 8-MOP in a track along cell nuclei. Irradiated cells were fixed with 2% paraformaldehyde supplemented with 0.1% Triton X-100 and washed in PBS buffer (PBS containing 0.15% glycine and 0.5% BSA) after which immunofluorescence was performed as described (28). Antibodies used were against CSB (E-18, 1:250, Santa Cruz, sc-10459), FANCD2 (FI-17, 1:1000, Novus Biologicals, nb100-316), XPA (FL-273, 1:100, Santa Cruz, sc-853), γH2AX (JBW301, 1:1000, Millipore, 05-636). Secondary antibodies were conjugated with Alexa Fluor

488, 555 and 633 (Invitrogen). DAPI vectashield (Vector Laboratories) was used to mount coverslips. Slides were imaged using an LSM700 confocal microscope (Zeiss).

Reactive oxygen species evaluation

Levels of cellular reactive oxygen species (ROS) were determined by quantifying the oxidation rate of H_2DCFDA (Invitrogen). VH10 cells were grown on 24 mm coverslips and treated with 100 μM oxaliplatin or cisplatin for 2 h, or with 10 mM H_2O_2 for 5 min. Next, cells were incubated with 10 μM H_2DCFDA in serum-free medium for 30 min, PBS washed and incubated with fresh serum-containing medium. H_2DCFDA fluorescence was measured by live cell imaging using an SP5 confocal laser-scanning microscope (Leica) and quantified with ImageJ software.

Recovery of RNA synthesis

Recovery of RNA synthesis (RRS) was measured by quantifying 5-ethynyl uridine (EU) incorporation in RNA in DLD-1 WT and KO cells grown on 24 mm coverslips and treated with 100 μM oxaliplatin or cisplatin for 2 h. Untreated cells and cells immediately after treatment, or after 6 or 22 h, were incubated with 0.33 mM EU for 1 h, fixed in 3.7% paraformaldehyde and permeabilized with 0.5% Triton X-100 (Sigma-Aldrich). EU incorporation was visualized using click-it reaction cocktail containing Atto 594 Azide (60 μM, Atto Tec.), Tris–HCl (50 mM, pH 7.6), $CuSO_4.5H_2O$ (4 mM, Sigma-Aldrich) and ascorbic acid (10 mM, Sigma-Aldrich). Slides were imaged using an LSM700 confocal microscope (Zeiss) and EU levels quantified with ImageJ software.

Fluorescence recovery after photobleaching

Fluorescence recovery after photobleaching (FRAP), using an SP5 confocal laser-scanning microscope (Leica), was applied to measure mobility of YFP-CSB^{del} or XRCC1-YFP in untreated cells or, as indicated, in cells treated for 6 h with 100, 200 or 400 μM oxaliplatin or 100 or 200 μM cisplatin, 15 J/m^2 UV-C (254 nm) or for 5 min with 10 mM H_2O_2. Immediately after treatment, YFP fluorescence was monitored every 22 ms at 1400 Hz with a zoom of 12× in a strip of 512 × 16 pixels spanning the nucleus, until steady state fluorescence was reached. Next, the strip was photobleached at maximum laser intensity. Fluorescence recovery was recorded using low laser intensity every 22 ms until steady-state levels were reached. Measurements were background-corrected and normalized to average prebleach fluorescence levels set at 100%. At least two independent experiments of >12 cells each were performed for each condition. The immobile fraction (F_{imm}) of each condition was determined by normalizing measurements to fluorescence intensity immediately after bleaching (I_0) and average fluorescence once recovery was complete in untreated cells ($I_{final,\ untr}$) and treated cells ($I_{final,\ treat}$), using the formula: $F_{imm} = 1 - (I_{final,\ treat} - I_{0,\ treat})/(I_{final,\ untr} - I_{0,\ treat})$ (29).

Statistics

Statistical differences were calculated using an unpaired one-tailed Student's *t*-test.

RESULTS

Multiple DNA repair pathways collectively protect cells against oxaliplatin

To characterize the exact DDR that acts in response to oxaliplatin, we used a loss-of-function CRISPR/Cas9 approach to screen for genes of the major DNA repair pathways that are required for survival of oxaliplatin-treated colorectal cancer cells. Forty-three genes encoding core proteins involved in the BER, NER, FA, HR, NHEJ and TLS pathways were selected (Supplementary Table S1). For all genes, except *XPA*, two sgRNAs were designed based on the following criteria: (i) complementarity to two early exons and not spanning the translation start sites, (ii) the lowest predicted off-target value, and (iii) the lowest number of single nucleotide polymorphisms in the target sequence. For *XPA*, a single sgRNA previously confirmed to induce a high KO efficiency, was used. To first determine the KO efficiency of designed sgRNAs, we tested 24 sgRNAs for their ability to induce indels in their respective target genes. sgRNAs and Cas9 were introduced by lentiviral transduction in DLD-1 cells and indel frequency was determined using TIDE analysis (27). This showed that efficiency of gene disruption by at least half of the designed sgRNAs was high and that these sgRNAs induced indels in over 40% of target sequences (Supplementary Table S2). These data provided sufficient proof of concept to proceed by using two sgRNAs per gene for achieving sufficient knockdown for our screening purpose.

All designed sgRNAs (Supplementary Table S1) were transduced together with Cas9 into DLD-1 cells such that 85 cell populations each expressing a unique sgRNA were established. Next, sensitivity of each cell population to an IC_{20} of oxaliplatin (15 μM) was determined using MTT viability assays. Only sgRNAs that conferred more that 50% cell death (i.e. >2-fold higher than WT DLD-1 cells) in two independent survival screens were considered as candidates for further validation. Among these, sgRNAs targeting genes involved in BER (*POLB, POLL* and *XRCC1*), NER (*CSA*, *XPF* and *ERCC1*), FA (*FANCA*, *FAAP24*, *SLX4*, *XPF* and *ERCC1*), HR (*MRE11*, *RAD50*, *RAD51, BRCA1* and *BRCA2*) and TLS (*REV3*) were identified as top hits (Figure 1A), showing that oxaliplatin lesions are likely processed by multiple DDR pathways. Given the well-established role of FA and HR in the removal of ICLs (13), the identification of several genes involved in these pathways confirmed the validity of the screen. Also, loss of the REV3 subunit of Polζ TLS polymerase, which is thought to act in the FA pathway, was shown before to confer strong sensitivity to ICL-inducing agents (30,31). Likewise, loss of ERCC1/XPF endonuclease activity, which is critical for both the NER and FA pathways (14,15,32), was expected to lead to strong oxaliplatin sensitivity. However, to our surprise, sgRNA targeting the TC-NER gene *CSA* strongly sensitized cells to oxaliplatin to the same degree as sgRNAs targeting *ERCC1/XPF* and HR and FA genes. Intriguingly, the same strong oxaliplatin hypersensitivity was observed in cells expressing sgRNAs against BER genes *POLB, POLL* (also implicated in NHEJ) and *XRCC1* (also implicated in NER). These results suggest that multiple

DNA repair pathways, including BER and TC-NER, act together to protect cells against oxaliplatin-induced DNA damage. Given the poorly defined role of TC-NER and BER in response to platinum drugs, we focused on elucidating their activity in response to oxaliplatin and, in comparison, to cisplatin.

Transcription-coupled NER resolves transcription block in platinum-treated cells

To verify the role of TC-NER, clonal DLD-1 cell lines stably depleted of TC-NER initiation factors CSA and CSB and downstream core NER factor XPF were generated, following sgRNA and Cas9 transfection (Figure 2A). We did not identify *CSB* in the screen but noticed that the sgRNAs we used yielded variable and low KO efficiency (Supplementary Figure S1), which is why for the stable *CSB* KO we designed new sgRNAs (see material and methods). MTT viability assays confirmed that loss of TC-NER, i.e. loss of either CSA or CSB, leads to strong sensitivity to oxaliplatin, as well as to cisplatin, similar as loss of NER in general, represented by XPF (Figure 2B and C). We corroborated these results using clonogenic survival assays with GG-NER-deficient *XP-C* and TC-NER-deficient *CS-B* fibroblasts, derived from xeroderma pigmentosum and Cockayne syndrome patients, respectively. As expected, both cell types were strongly sensitive to UV (Figure 2D). Strikingly, however, TC-NER-deficient fibroblasts exhibited a much stronger sensitivity to oxaliplatin than GG-NER-deficient fibroblasts (Figure 2E). These results suggest that cells largely rely on TC-NER activity, and to a lesser extent on GG-NER, to overcome the cell killing effect of platinum DNA lesions.

As TC-NER removes DNA damage that blocks RNAP2 elongation, recovery of RNA synthesis (RRS) after DNA damage induction is commonly used as an indirect indicator of TC-NER activity (33). We therefore measured RNA synthesis in WT and CSA KO DLD-1 cells at different time points after oxaliplatin and cisplatin treatment by quantifying incorporation of EU into *de novo* synthesized RNA. Oxaliplatin and cisplatin both effectively inhibited transcription, which in WT cells recovered fully after 24 h (Figure 3A–D). In contrast, transcription recovery in CSA KO cells was incomplete after 24 h. These data indicate that both platinum drugs impair transcriptional activity of cancer cells, hampering cell function and proliferation if transcription-blocking platinum lesions are not removed by TC-NER.

CSB binds damaged chromatin in platinum-treated cells depending on transcription

To further confirm the initiation of TC-NER in response to platinum lesions in living cells, we tested whether the essential TC-NER factor CSB binds to damaged chromatin after oxaliplatin or cisplatin treatment. To this end, we measured mobility of YFP-tagged CSB by means of fluorescence recovery after photobleaching (FRAP), as decreased mobility of DNA repair proteins after DNA damage infliction reflects their involvement in DNA repair (34). In response to UV irradiation, only a very small fraction of CSB immobilizes, likely due to transient DNA interaction and relatively few lesions that are substrate for TC-NER (35). Therefore, we used a CSB mutant protein that is not released from DNA damage because it lacks its C-terminal ubiquitin binding domain (hereafter referred to as CSB^{del}) (21). CSB^{del} was, in line with previous findings, strongly immobilized after UV irradiation, and, importantly, also after oxaliplatin or cisplatin exposure, in a dose-dependent manner (Figure 4A and B). In line with its role in TC-NER, UV-induced CSB^{del} chromatin binding is dependent on active transcription (21). Similarly, we could suppress the oxaliplatin- and cisplatin-induced CSB^{del} immobilization by inhibiting RNAP2 elongation using flavopiridol (36) (Figure 4B and Supplementary Figure S2). These results indicate that CSB becomes bound to damaged chromatin in response to oxaliplatin or cisplatin in a transcription-dependent manner, which therefore likely reflects its initiation of TC-NER.

To demonstrate participation of TC-NER in the response to DNA crosslinks in another manner than through platinum drug exposure, we tested recruitment of CSB to intra- and interstrand crosslinks induced by UVA-activated 8-MOP in living cells. To this end, U2OS and YFP-CSB^{del} expressing cells were treated with 8-MOP and irradiated in a local subnuclear region using a 355 nm UVA laser (17). We observed clear recruitment of FANCD2, an essential recognition factor within the FA pathway, and XPA, a central coordinator of the NER pathway, to local laser-induced DNA damage, as visualized by γH2AX staining (Figure 4C). Recruitment of these factors suggested that both intra- and interstrand crosslinks were efficiently induced using this method. Notably, CSB^{del} was also strongly recruited to these DNA damage sites generated by UVA-activated 8-MOP, supporting the idea that DNA crosslinks lead to initiation of TC-NER. Taken together, our results suggest that DNA crosslinking agents strongly and negatively impact transcriptional activity of cells and emphasize the importance of TC-NER for survival of cells exposed to these agents.

Base excision repair is required for resolving platinum drug-induced transcription blockage

To verify the rather surprising involvement of BER in the response to platinum drug exposure, we established stable KO clonal DLD-1 cell lines of core BER factors XRCC1, PARP1 and POLB (Figure 5A). MTT assays with these KO cells confirmed that functional loss of BER leads to increased sensitivity to oxaliplatin (Figure 5B) as well as to cisplatin (Figure 5C). Similarly, cells pre-treated with PARP inhibitor olaparib or POLB inhibitor pamoic acid showed hypersensitivity to both drugs (Figure 5D and E), implying that indeed BER protects cells against platinum drug treatment. Since platinum drugs have a profound inhibitory effect on transcription, we tested whether BER, like TC-NER, is necessary for alleviating platinum drug-induced transcription interference, by performing RRS. Strikingly, both POLB KO DLD-1 cells as well as DLD-1 cells treated with POLB inhibitor pamoic acid showed impaired transcription recovery 24 h after oxaliplatin or cisplatin exposure (Figure 5F–I). These data point to the relevance of

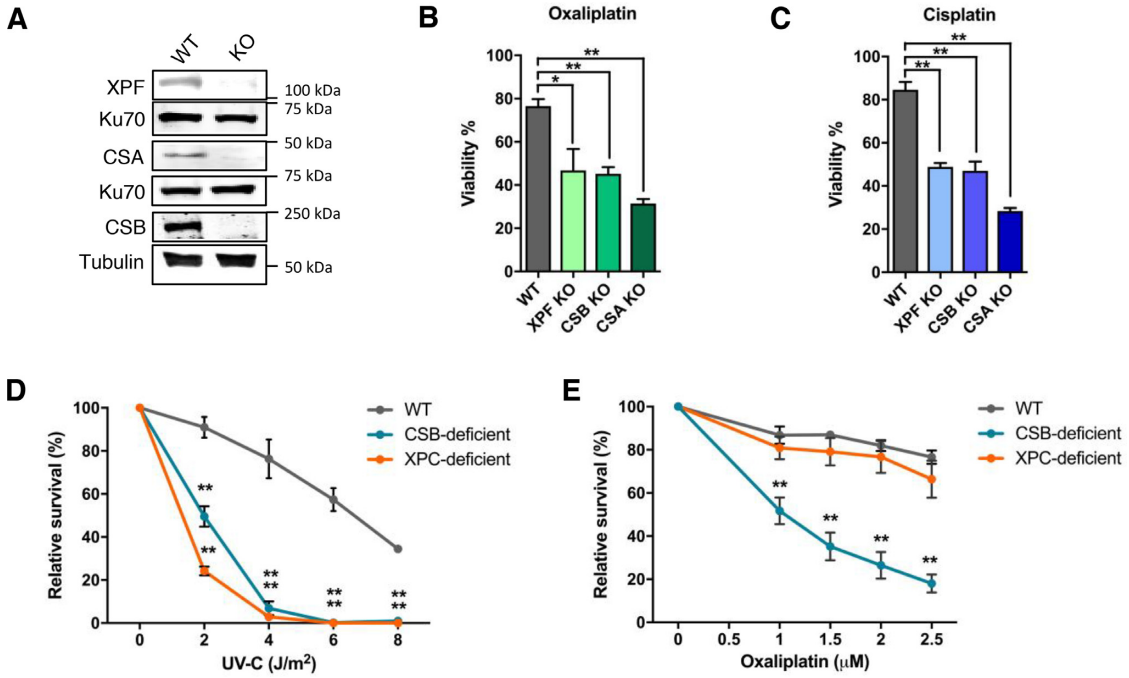

Figure 2. Cells deficient in transcription-coupled NER are sensitive to platinum drugs. (**A**) Immunoblot showing loss of XPF, CSA and CSB protein expression in stable knockout (KO) DLD-1 cells as compared to wild type (WT) cells. Ku70 and Tubulin were used as loading controls. (**B**) MTT assay showing sensitivity of NER-deficient KO cells to 15 μM oxaliplatin. (**C**) MTT assay showing sensitivity of NER-deficient KO cells to 10 μM cisplatin. Cell viability in (B) and (C) was measured 3 days after drug treatment. Bars denote mean and SEM of 2 independent experiments each performed in triplicate. (**D**) Response of NER-proficient human C5RO fibroblasts (WT), TC-NER-deficient CS1AN fibroblasts (CSB-deficient) and GG-NER-deficient XP4PA fibroblasts (XPC-deficient) to UV-C irradiation and (**E**) oxaliplatin. Each experimental point represents mean and SEM of 3 (D) or 6 (E) independent experiments, each performed in triplicate. For all panels, $*P < 0.05$; $**P < 0.01$

BER in maintaining transcriptional integrity in cells exposed to platinum drugs.

XRCC1 chromatin binding in platinum-treated cells is partially dependent on transcription

To show that BER is activated upon exposure to platinum drugs, we used FRAP to determine chromatin binding of YFP-tagged XRCC1 in oxaliplatin and cisplatin-treated cells. We first determined XRCC1 mobility in cells treated with H_2O_2, a potent generator of oxidative lesions that are substrates for BER (37). As expected, H_2O_2 induced a strong XRCC1 immobilization, indicative of BER activity (Figure 6A). Likewise, we observed clear XRCC1 immobilization upon treatment with oxaliplatin or cisplatin. This oxaliplatin- and cisplatin-induced XRCC1 immobilization was reduced in the presence of RNAP2 inhibitor flavopiridol (Figure 6A), suggesting that XRCC1-involved BER activity in response to platinum drug exposure is partially dependent on active transcription. XRCC1 partners with DNA ligase III and functions in the final ligation step of BER (38) but possibly also of NER in non-proliferating cells (39). To discern between its activity in BER and NER in response to platinum drugs, we measured XRCC1 mobility after RNAi-mediated knockdown of the main BER glycosylase OGG1 and the NER factor XPA (Supplementary Figure S3A-B), both acting upstream of XRCC1. As shown in Figure 6B, XRCC1 immobilization was for the most part dependent on OGG1 and not XPA, suggesting that oxaliplatin exposure leads to XRCC1 engagement in a glycosylase-dependent BER pathway.

Platinum drugs generate oxidative damage

BER is well known to recognize subtle nucleobase modifications like oxidations. Some DNA glycosylases have also been implicated in repair of different types of DNA crosslinks (40–43). However, the observation that platinum drug-induced XRCC1 chromatin binding is dependent on OGG1 is striking, because this glycosylase is mainly known to have affinity for 8-oxoG oxidative lesions and not for DNA crosslinks (8). Therefore, we determined whether platinum drug exposure could lead to oxidative DNA damage induction that would require BER for its removal, by testing whether oxaliplatin and cisplatin treatment might lead to generation of ROS. ROS production was evaluated using the fluorescent ROS indicator H_2DCFDA (44), in slowly dividing VH10 fibroblasts grown in low oxygen. ROS generation by H_2O_2 exposure, as control, led to strong induction of H_2DCFDA fluorescence (Figure 6C). Interestingly, also oxaliplatin and cisplatin treatment increased H_2DCFDA fluorescence, suggesting that exposure to these platinum drugs leads to intracellular ROS production. To test whether BER is indeed initiated by oxidative damage generated after platinum drug exposure, we measured XRCC1 mobility in H_2O_2 and platinum drug-treated cells following pre-treatment with the antioxidant trolox. Trolox pre-treatment significantly reduced ROS production after

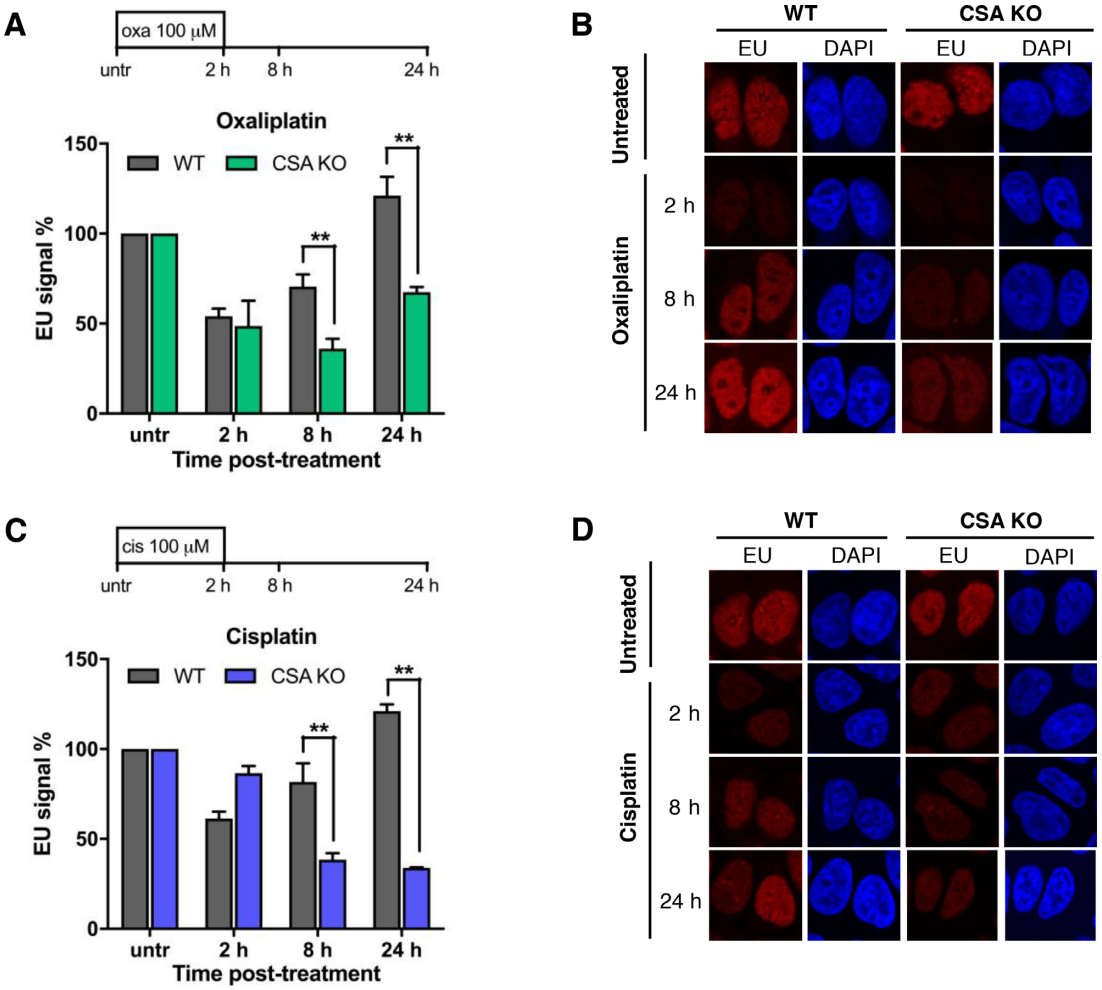

Figure 3. Transcription-coupled NER is required for transcription recovery in platinum-treated cells. (**A**) Recovery of RNA synthesis (RRS), as determined by quantification of EU incorporation at the indicated time points, in DLD-1 wild type (WT) and CSA knockout (CSA KO) cells after 2 h treatment with 100 μM of oxaliplatin. (**B**) Representative pictures of the oxaliplatin RRS. (**C**) RRS in DLD-1 WT and CSA KO cells after 2 h treatment with 100 μM of cisplatin. (**D**) Representative pictures of the cisplatin RRS. Bars represent mean EU signal and SEM of >100 cells from two independent experiments normalized to untreated control for each cell line, set at 100%. For all panels, $*P < 0.05$; $**P < 0.01$

H_2O_2 exposure (Supplementary Figure S4) and also significantly reduced H_2O_2-dependent XRCC1 immobilization (Figure 6D). In a similar manner, trolox pre-treatment significantly reduced ROS production after oxaliplatin and cisplatin exposure (Supplementary Figure S4) and decreased platinum drug-induced XRCC1 immobilization. These observations indicate that exposure of cells to platinum drugs not only induces DNA crosslinks that impair cellular function, but also leads to generation of oxidative DNA lesions via ROS production. This likely explains why BER protects cells against platinum drug exposure.

DISCUSSION

Cisplatin is widely administered as standard chemotherapeutic agent in cancer treatment, but was replaced by the more effective oxaliplatin in treatment of advanced colorectal cancer (CRC) (1). CRC is associated with increased chromosomal or microsatellite instability, the latter being caused by defective DNA mismatch repair (MMR). We expected that CRISPR/Cas9 gene editing would be less efficient in chromosomally unstable cells than in MMR-deficient cells, due to their intrinsic aneuploidy and copy number variations. We therefore chose MMR-deficient DLD-1 cells for our loss-of-function screen. MMR itself does not appear to be involved in the DDR to oxaliplatin (45), which is why MMR genes were also not included in the screen. Our screening suggests that an intricate DDR response protects CRC cells against oxaliplatin, involving multiple DNA repair pathways including FA, HR, TLS, TC-NER and BER, which likely results from the large spectrum of lesions induced by this drug. Oxaliplatin, as well as cisplatin, covalently binds to DNA to form various DNA crosslinks, such as Pt-GpG (60–65%), Pt-ApG (25–30%), Pt-GNG (5–10%) and ICLs (1–6%), in addition to monofunctional adducts (2%) and DNA-protein crosslinks (1–3,46). It is therefore not surprising that genes from all repair pathways known to deal with DNA crosslinks, namely FA, HR, TLS and NER, were identified. Nevertheless, the specific identification of *CSA*, essential for TC-NER, but not *XPC* or *DDB2,*

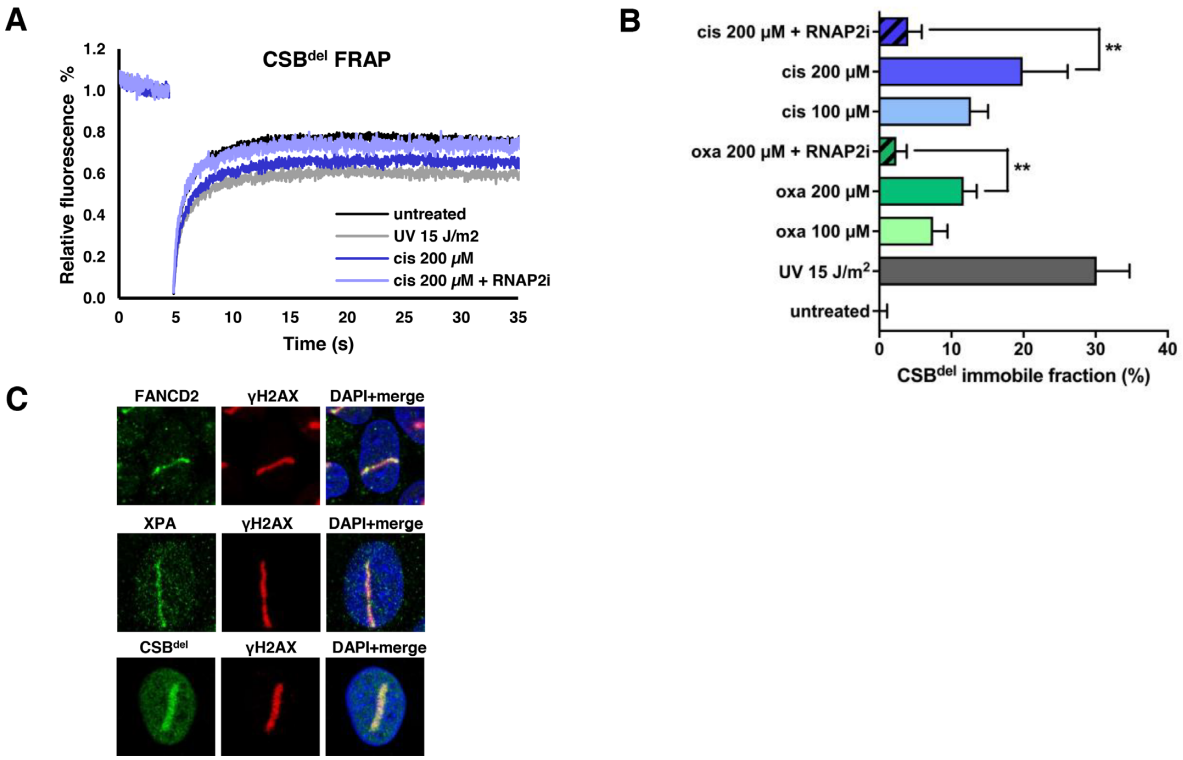

Figure 4. CSB is recruited to chromatin in platinum-treated cells in a transcription-dependent manner. (**A**) Fluorescence recovery after photobleaching (FRAP) analysis of YFP-CSB^{del}, showing reduced mobility after 15 J/m^2 UV-C or 200 μM cisplatin (cis; applied for 6 h), depending on transcription which was blocked by RNA polymerase II inhibitor (RNAP2i) flavopiridol (1 μM applied for 1 h). The reduced mobility represents the fraction of CSB bound to chromatin and involved in active DNA repair. (**B**) Percentage immobile fraction, i.e. chromatin-bound fraction, of CSB^{del} after DNA damage induction as determined by FRAP analyses such as shown in (A). Cells were irradiated with 15 J/m^2 UV-C or treated for 6 h with either 100 or 200 μM oxaliplatin (oxa) or cisplatin (cis) without or with 1 h pre-treatment with 1 μM RNA polymerase II inhibitor (RNAP2i) flavopiridol, as indicated. Bars represent mean and SEM of at least 24 cells analyzed in 2 independent experiments. (**C**) Immunofluorescence showing localization of FANCD2, XPA and YFP-CSB^{del} to sites of intra- and interstrand crosslinks (visualized by γH2AX staining), introduced by UVA-laser activation of 8-methoxypsoralen (50 μM). For all panels, $*P < 0.05$; $**P < 0.01$

essential for GG-NER, was striking. This suggests that TC-NER, and thus transcriptional integrity, is more important to cellular survival after oxaliplatin exposure than GG-NER. This was further confirmed by our oxaliplatin survival experiments with patient-derived NER-deficient fibroblasts, which, in line with previously reported similar cisplatin survival experiments (16,47,48), shows that TC-NER-deficient cells are sensitive to platinum drugs but GG-NER-deficient cells are not.

The interference of ICLs with replication is often considered as the major cytotoxic mechanism through which platinum drugs exert their anti-tumor efficacy. Our results, however, emphasize that oxaliplatin and cisplatin both strongly suppress transcription as well, in line with previous literature (49–51) and that functional TC-NER is critical to overcome this transcription block. Thus, platinum drug cytotoxicity may as well be exerted through inhibition of transcription, as is also suggested before (2). Notably, the oxaliplatin and cisplatin sensitivity of TC-NER-deficient *CSA* and *CSB* knockout CRC cells was equal to that of cells knockout for *XPF*, i.e which lack functional GG- and TC-NER and ICL repair due to XPF's critical role in these pathways (15,32). This highlights the relevance of TC-NER in platinum drug resistance. CSB^{del} was immobilized by both oxaliplatin and cisplatin and recruited to damage generated by UVA-activated 8-MOP, similar as previously observed for UVA-activated trioxsalen (52). From these experiments, it cannot be distinguished whether CSB acts on either platinum–DNA intrastrand crosslinks or ICLs or on both. As plasmid-based reporter assays in human cells have shown that platinum-DNA intrastrand crosslinks block RNAP2 (53) and that replication-independent repair of cisplatin-ICLs specifically depends on CSB (16), it is likely that TC-NER acts on both types of lesions (Figure 7). Platinum drugs also crosslink proteins to DNA (46), which may interfere with transcription (54). Recently, a new repair pathway was identified that proteolytically processes these DNA-protein crosslinks, leaving a small peptide-DNA remnant that could possibly be repaired by NER (55–57). It would be interesting to determine whether TC-NER, rather than GG-NER, acts specifically on such substrates as well.

A role for BER in resistance of cancer cells to platinum drugs has previously been suggested (58–62). However, our observation that in isogenic cells BER appears equally critical as other DDR pathways indicates that the importance of BER in protecting against platinum drugs may be generally underappreciated. PARP1, XRCC1 and POLB, whose inactivation rendered cells hypersensitive to oxaliplatin and cisplatin, have been implicated in other repair pathways besides BER as well (39,63–65). Therefore, their involvement

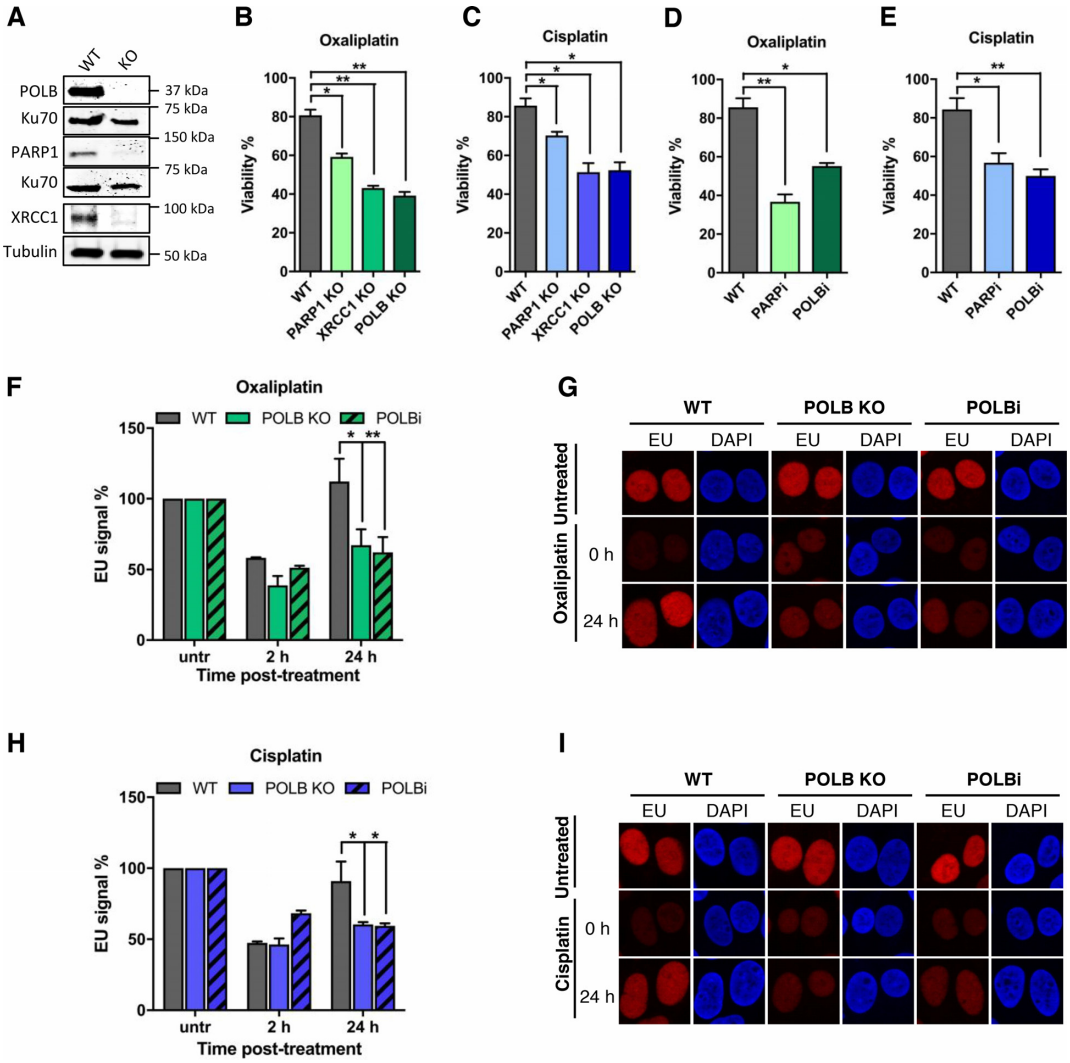

Figure 5. Base excision repair helps to resolve platinum-induced transcription blockage. (**A**) Immunoblot showing loss of POLB, PARP1 and XRCC1 protein expression in stable knockout (KO) DLD-1 cells as compared to wild type (WT) cells. Ku70 and Tubulin were used as loading controls. (**B**) MTT assay showing sensitivity of BER-deficient KO cells to 15 μM oxaliplatin. (**C**) MTT assay showing sensitivity of BER-deficient KO cells to 10 μM cisplatin. (**D** and **E**) MTT assays showing sensitivity of DLD-1 cells treated with 10 μM of PARP inhibitor olaparib (PARPi) or 500 μM POLB inhibitor pamoic acid (POLBi) to 15 μM oxaliplatin or 10 μM cisplatin, respectively. Cell viability in (B-E) was measured 3 days after drug treatment. Bars denote mean and SEM of 2 independent experiments each performed in triplicate. (**F**) Recovery of RNA synthesis (RRS) in DLD-1 wild type (WT) and BER-deficient cells, either by POLB knockout (KO) or by application of the POLB inhibitor pamoic acid (POLBi). EU incorporation was quantified at the indicated time points following 2 h treatment with 100 μM of oxaliplatin. (**G**) Representative pictures of the oxaliplatin RRS. (**H**) RRS in DLD-1 WT and BER-deficient cells exposed to 100 μM of cisplatin for 2 h. (**I**) Representative pictures of the cisplatin RRS. Bars represent mean EU signal and SEM of >100 cells from 2 independent experiments normalized to untreated control for each cell line, set at 100%. Figures show representative RRS pictures. For all panels, * $P < 0.05$; ** $P < 0.01$

may not necessarily imply that (only) BER is engaged in response to platinum drugs. However, BER involvement was confirmed by the fact that platinum drug-induced immobilization of XRCC1 was predominantly dependent on OGG1, a glycosylase exclusively implicated in BER (66). Some DNA glycosylases, like NEIL1 and NEIL3, have been shown to recognize and cleave psoralen-induced ICLs (40,42,43) and also the MPG glycosylase has been implicated in protection against ICL induction by various crosslinking agents (41,67). Possibly, OGG1 may also recognize platinum-induced DNA crosslinks and BER could protect against platinum drugs by recognizing and removing platinum-DNA lesions via OGG1. However, in agreement with previous reports (68–70), we found that both oxaliplatin and cisplatin exposure leads to strongly increased intracellular ROS levels, likely as a consequence of damage to mitochondria (71) or an interaction with DNA (72) or glutathione (73). Importantly also, platinum drug-induced XRCC1 immobilization could be suppressed by antioxidant pre-treatment. This, together with dependence on OGG1, which is well known as glycosylase dealing with 8-oxoG oxidative lesions that are predominantly formed when cells are exposed to oxidative stress (8), suggests that BER mainly protects against platinum drug cytotoxicity by removing oxidative DNA lesions (Figure 7).

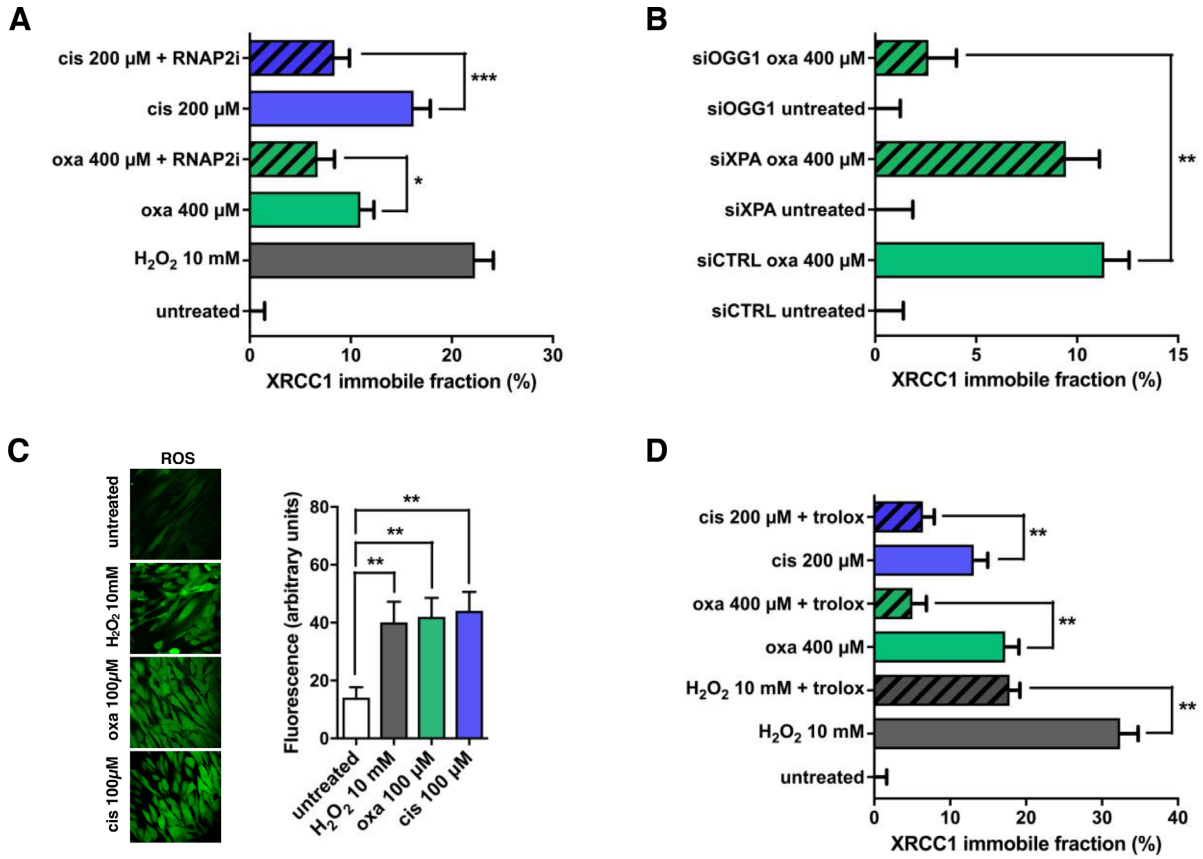

Figure 6. XRCC1 chromatin retention upon platinum treatment is partially dependent on transcription. (**A**) Percentage XRCC1-YFP immobile fraction, i.e. chromatin-bound fraction, as determined by FRAP in MRC-5 cells, after treatment for 5 min with 10 mM hydrogen peroxide (H_2O_2), 6 h with 400 µM oxaliplatin (oxa), 6 h with 200 µM cisplatin (cis) without or with 1 h pre-treatment with 1 µM RNA Polymerase II inhibitor (RNAP2i) flavopiridol, as indicated. Bars represent mean and SEM of at least 24 cells analyzed in two independent experiments. (**B**) Percentage XRCC1-YFP immobile fraction determined by FRAP after 6 h exposure to 400 µM oxaliplatin of MRC-5 cells treated with control siRNA (siCTRL) and siRNA against XPA (siXPA) and OGG1 (siOGG1). Bars represent mean and SEM of at least 24 cells analyzed in 2 independent experiments. (**C**) Induction of reactive oxygen species (ROS) by 10 mM H_2O_2 applied for 5 min, and 100 µM oxaliplatin or cisplatin applied for 6 h in VH10 cells, as measured by H_2DCFDA fluorescence. Figure shows representative confocal pictures and quantification of fluorescence signal of >100 cells from 2 independent experiments represented by the mean and SEM. (**D**) Percentage XRCC1-YFP immobile fraction, as determined by FRAP in MRC-5 cells, after treatment for 5 min with 10 mM H_2O_2, 6 h with 400 µM oxaliplatin (oxa) or 6 h with 200 µM cisplatin (cis) without or with 24 h pre-treatment with 600 µM trolox, as indicated. Bars represent mean and SEM of at least 24 cells analyzed in two independent experiments. For all panels, $*P < 0.05$; $**P < 0.01$; $***P < 0.001$

Intriguingly, platinum drug-induced XRCC1 immobilization was partially dependent on transcription and platinum drug-induced transcription arrest was only recovered in the presence of functional BER. This suggests that BER is needed to eliminate DNA lesions that interfere with transcription. Nonetheless, apart from sporadic cyclopurines, it is still debated whether the majority of oxidative lesions, including 8-oxoG, can effectively block RNAP2 (74–79). It may also be that intermediate BER products, such as single-strand breaks and abasic sites, constitute the real barrier to transcription (74,80) (Figure 7). Apart from acting directly on platinum-DNA crosslinks, the TC-NER protein CSB may have a role in resolving these transcription blocks as well, as CSB is recruited to oxidative lesions in a transcription-dependent manner (81), to promote XRCC1 recruitment (82).

Based on our analysis, we conclude that interference with transcriptional integrity is one of the major cytotoxic effects of platinum drugs. Recently, differences in cytotoxicity profile and clinical application of oxaliplatin and cisplatin were attributed to differences in cell killing mechanisms, with cisplatin being classified as DNA crosslinker and oxaliplatin as transcription/translation inhibitor, killing cells through ribosome biogenesis stress (83). We did not observe obvious differences between both drugs in transcription inhibition and TC-NER or BER involvement. It is not exactly known whether platinum drugs inhibit RNA polymerase I, but TC-NER proteins CSA and CSB have both been implicated in RNA polymerase I transcription of rRNA (84,85). It is therefore likely that TC-NER is also necessary for repair of RNA Polymerase I transcription-blocking lesions explaining why oxaliplatin exposure leads to ribosome biogenesis stress. In any scenario, cancer cells are strongly dependent on the function of TC-NER and BER to overcome transcription stress. This may be of clinical relevance, as tumor relapse after chemotherapy is attributed to intrinsically resistant and quiescent-like cancer stem cells refractory to treatment (86). Since such cells do not rapidly proliferate, they may be more susceptible to transcription interference than to replication arrest and may therefore rely

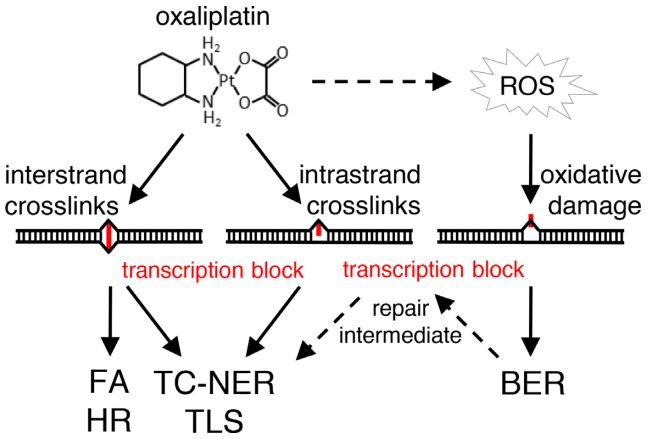

Figure 7. Model depicting the DNA damage response to platinum drug exposure. Platinum drugs like cisplatin and oxaliplatin induce DNA interstrand and intrastrand crosslinks and lead to the production of reactive oxygen species (ROS) that induce oxidative lesions. Bulky DNA crosslinks can directly block RNA polymerase II, inhibiting transcription, and need to be dealt with by Fanconi anemia (FA), homologous recombination (HR), transcription-coupled nucleotide excision repair (TC-NER) and translesion synthesis (TLS) DNA repair and tolerance pathways. Oxidative lesions are processed by base excision repair (BER). Transcription is inhibited either directly by oxidative lesions or by BER intermediate abasic sites or single-strand breaks.

more on DNA repair processes like TC-NER and BER that maintain transcription. Furthermore, a major drawback of the clinical application of platinum drugs is their acute and chronic side toxicity, in particular to post-mitotic cells like peripheral neurons, limiting treatment dose and duration (87). Importantly, cisplatin and oxaliplatin were found to accumulate in DNA in rat peripheral neurons *in vivo,* strongly inhibiting transcription (88,89). This, together with the notion that transcription defects lead to neuronal degeneration (11) indicates that transcription impairment by platinum-DNA adducts is a plausible cause for their specific side toxicity to post-mitotic cells. It would therefore be beneficial to better understand exact transcription-coupled DDR mechanisms in cancer stem cells and post-mitotic neuronal cells, to be able to improve efficacy of platinum drug treatment and prevent unwanted side effects.

SUPPLEMENTARY DATA

Supplementary Data are available at NAR Online.

ACKNOWLEDGEMENTS

The authors are thankful to Jurgen Marteijn and Roel Janssens for providing sequences for some of the sgRNAs, Orlando Schärer for critical reading of the manuscript and Erasmus MC Optical Imaging Centre for technical support with microscopes.

FUNDING

European Research Council Advanced Grant [340988-ERC ID to W.V.]; Dutch Cancer Society [KWF grant 10506 to W.V.]; FP7 Marie Curie International Training Network aDDRess [316390 M.S. and C.R.S.]; Worldwide Cancer Research [15-1274]. J.S. was awarded by EMBO long-term fellowship [ALTF 663-2014]; Oncode Institute which is partly financed by the Dutch Cancer Society and was funded by the gravitation program CancerGenomiCs.nl from the Netherlands Organisation for Scientific Research (NWO). Funding for open access charge: European Research Council.

Conflict of interest statement. None declared.

REFERENCES

1. Kelland,L. (2007) The resurgence of platinum-based cancer chemotherapy. *Nat. Rev. Cancer*, **7**, 573–584.
2. Riddell,I.A. (2018) Cisplatin and oxaliplatin: our current understanding of their actions. *Met. Ions Life Sci.*, **18**, 1–42.
3. Jung,Y. and Lippard,S.J. (2007) Direct cellular responses to platinum-induced DNA damage. *Chem Rev.*, **107**, 1387–1407.
4. Koberle,B., Masters,J.R., Hartley,J.A. and Wood,R.D. (1999) Defective repair of cisplatin-induced DNA damage caused by reduced XPA protein in testicular germ cell tumours. *Curr. Biol.: CB*, **9**, 273–276.
5. Welsh,C., Day,R., McGurk,C., Masters,J.R., Wood,R.D. and Koberle,B. (2004) Reduced levels of XPA, ERCC1 and XPF DNA repair proteins in testis tumor cell lines. *Int. J. Cancer*, **110**, 352–361.
6. Giglia-Mari,G., Zotter,A. and Vermeulen,W. (2011) DNA damage response. *Cold Spring Harb. Perspect. Biol.*, **3**, a000745.
7. Jackson,S.P. and Bartek,J. (2009) The DNA-damage response in human biology and disease. *Nature*, **461**, 1071–1078.
8. Krokan,H.E. and Bjoras,M. (2013) Base excision repair. *Cold Spring Harb. Perspect. Biol.*, **5**, a012583.
9. Dianov,G.L. and Hubscher,U. (2013) Mammalian base excision Repair: the forgotten archangel. *Nucleic Acids Res.*, **41**, 3483–3490.
10. Scharer,O.D. (2013) Nucleotide excision repair in eukaryotes. *Cold Spring Harb. Perspect. Biol.*, **5**, a012609.
11. Marteijn,J.A., Lans,H., Vermeulen,W. and Hoeijmakers,J.H. (2014) Understanding nucleotide excision repair and its roles in cancer and ageing. *Nat. Rev. Mol. Cell Biol.*, **15**, 465–481.
12. Ceccaldi,R., Rondinelli,B. and D'Andrea,A.D. (2016) Repair pathway choices and consequences at the double-strand break. *Trends Cell Biol.*, **26**, 52–64.
13. Clauson,C., Scharer,O.D. and Niedernhofer,L. (2013) Advances in understanding the complex mechanisms of DNA interstrand cross-link repair. *Cold Spring Harb. Perspect. Biol.*, **5**, a012732.
14. Bhagwat,N., Olsen,A.L., Wang,A.T., Hanada,K., Stuckert,P., Kanaar,R., D'Andrea,A., Niedernhofer,L.J. and McHugh,P.J. (2009) XPF-ERCC1 participates in the Fanconi anemia pathway of cross-link repair. *Mol. Cell. Biol.*, **29**, 6427–6437.
15. Klein Douwel,D., Boonen,R.A., Long,D.T., Szypowska,A.A., Raschle,M., Walter,J.C. and Knipscheer,P. (2014) XPF-ERCC1 acts in unhooking DNA interstrand crosslinks in cooperation with FANCD2 and FANCP/SLX4. *Mol. Cell*, **54**, 460–471.
16. Enoiu,M., Jiricny,J. and Scharer,O.D. (2012) Repair of cisplatin-induced DNA interstrand crosslinks by a replication-independent pathway involving transcription-coupled repair and translesion synthesis. *Nucleic Acids Res.*, **40**, 8953–8964.
17. Muniandy,P.A., Thapa,D., Thazhathveetil,A.K., Liu,S.T. and Seidman,M.M. (2009) Repair of laser-localized DNA interstrand cross-links in G1 phase mammalian cells. *J. Biol. Chem.*, **284**, 27908–27917.
18. Bowden,N.A. (2014) Nucleotide excision repair: why is it not used to predict response to platinum-based chemotherapy? *Cancer Lett.*, **346**, 163–171.
19. Dayagrosjean,L., James,M.R., Drougard,C. and Sarasin,A. (1987) An immortalized xeroderma-pigmentosum, group-C, cell-line which replicates Sv40 shuttle vectors. *Mut. Res.*, **183**, 185–196.
20. Mayne,L.V., Priestley,A., James,M.R. and Burke,J.F. (1986) Efficient immortalization and morphological transformation of human-fibroblasts by transfection with Sv40 DNA linked to a dominant marker. *Exp. Cell Res.*, **162**, 530–538.
21. Anindya,R., Mari,P.O., Kristensen,U., Kool,H., Giglia-Mari,G., Mullenders,L.H., Fousteri,M., Vermeulen,W., Egly,J.M. and

Svejstrup,J.Q. (2010) A ubiquitin-binding domain in cockayne syndrome B required for transcription-coupled nucleotide excision repair. *Mol. Cell*, **38**, 637–648.
22. Amouroux,R., Campalans,A., Epe,B. and Radicella,J.P. (2010) Oxidative stress triggers the preferential assembly of base excision repair complexes on open chromatin regions. *Nucleic Acids Res.*, **38**, 2878–2890.
23. Campeau,E., Ruhl,V.E., Rodier,F., Smith,C.L., Rahmberg,B.L., Fuss,J.O., Campisi,J., Yaswen,P., Cooper,P.K. and Kaufman,P.D. (2009) A versatile viral system for expression and depletion of proteins in mammalian cells. *PLoS One*, **4**, e6529.
24. Hsu,P.D., Scott,D.A., Weinstein,J.A., Ran,F.A., Konermann,S., Agarwala,V., Li,Y., Fine,E.J., Wu,X., Shalem,O *et al.*2013) DNA targeting specificity of RNA-guided Cas9 nucleases. *Nat. Biotechnol.*, **31**, 827–832.
25. Sanjana,N.E., Shalem,O. and Zhang,F. (2014) Improved vectors and genome-wide libraries for CRISPR screening. *Nat. Methods*, **11**, 783–784.
26. Dull,T., Zufferey,R., Kelly,M., Mandel,R.J., Nguyen,M., Trono,D. and Naldini,L. (1998) A third-generation lentivirus vector with a conditional packaging system. *J. Virol.*, **72**, 8463–8471.
27. Brinkman,E.K., Chen,T., Amendola,M. and van Steensel,B. (2014) Easy quantitative assessment of genome editing by sequence trace decomposition. *Nucleic Acids Res.*, **42**, e168.
28. Aydin,O.Z., Marteijn,J.A., Ribeiro-Silva,C., Lopez,A.R., Wijgers,N., Smeenk,G., van Attikum,H., Poot,R.A., Vermeulen,W. and Lans,H. (2014) Human ISWI complexes are targeted by SMARCA5 ATPase and SLIDE domains to help resolve lesion-stalled transcription. *Nucleic Acids Res.*, **42**, 8473–8485.
29. van Cuijk,L., van Belle,G.J., Turkyilmaz,Y., Poulsen,S.L., Janssens,R.C., Theil,A.F., Sabatella,M., Lans,H., Mailand,N., Houtsmuller,A.B. *et al.* (2015) SUMO and ubiquitin-dependent XPC exchange drives nucleotide excision repair. *Nat. Commun.*, **6**, 7499.
30. Nojima,K., Hochegger,H., Saberi,A., Fukushima,T., Kikuchi,K., Yoshimura,M., Orelli,B.J., Bishop,D.K., Hirano,S., Ohzeki,M. *et al.* (2005) Multiple repair pathways mediate tolerance to chemotherapeutic cross-linking agents in vertebrate cells. *Cancer Res.*, **65**, 11704–11711.
31. Raschle,M., Knipsheer,P., Enoiu,M., Angelov,T., Sun,J.C., Griffith,J.D., Ellenberger,T.E., Scharer,O.D. and Walter,J.C. (2008) Mechanism of replication-coupled DNA interstrand crosslink repair. *Cell*, **134**, 969–980.
32. Sijbers,A.M., de Laat,W.L., Ariza,R.R., Biggerstaff,M., Wei,Y.F., Moggs,J.G., Carter,K.C., Shell,B.K., Evans,E., de Jong,M.C. *et al.* (1996) Xeroderma pigmentosum group F caused by a defect in a structure-specific DNA repair endonuclease. *Cell*, **86**, 811–822.
33. Nakazawa,Y., Yamashita,S., Lehmann,A.R. and Ogi,T. (2010) A semi-automated non-radioactive system for measuring recovery of RNA synthesis and unscheduled DNA synthesis using ethynyluracil derivatives. *DNA Repair (Amst.)*, **9**, 506–516.
34. Vermeulen,W. (2011) Dynamics of mammalian NER proteins. *DNA Repair (Amst.)*, **10**, 760–771.
35. van den Boom,V., Citterio,E., Hoogstraten,D., Zotter,A., Egly,J.M., van Cappellen,W.A., Hoeijmakers,J.H., Houtsmuller,A.B. and Vermeulen,W. (2004) DNA damage stabilizes interaction of CSB with the transcription elongation machinery. *J. Cell Biol.*, **166**, 27–36.
36. Senderowicz,A.M. (1999) Flavopiridol: the first cyclin-dependent kinase inhibitor in human clinical trials. *Invest. New Drugs*, **17**, 313–320.
37. Ray,G. and Husain,S.A. (2002) Oxidants, antioxidants and carcinogenesis. *Indian J. Exp. Biol.*, **40**, 1213–1232.
38. Cappelli,E., Taylor,R., Cevasco,M., Abbondandolo,A., Caldecott,K. and Frosina,G. (1997) Involvement of XRCC1 and DNA ligase III gene products in DNA base excision repair. *J. Biol. Chem.*, **272**, 23970–23975.
39. Moser,J., Kool,H., Giakzidis,I., Caldecott,K., Mullenders,L.H. and Fousteri,M.I. (2007) Sealing of chromosomal DNA nicks during nucleotide excision repair requires XRCC1 and DNA ligase III alpha in a cell-cycle-specific manner. *Mol. Cell*, **27**, 311–323.
40. Martin,P.R., Couve,S., Zutterling,C., Albelazi,M.S., Groisman,R., Matkarimov,B.T., Parsons,J.L., Elder,R.H. and Saparbaev,M.K. (2017) The Human DNA glycosylases NEIL1 and NEIL3 Excise Psoralen-Induced DNA-DNA Cross-Links in a Four-Stranded DNA Structure. *Scientific Rep.*, **7**, 17438.
41. Allan,J.M., Engelward,B.P., Dreslin,A.J., Wyatt,M.D., Tomasz,M. and Samson,L.D. (1998) Mammalian 3-methyladenine DNA glycosylase protects against the toxicity and clastogenicity of certain chemotherapeutic DNA cross-linking agents. *Cancer Res.*, **58**, 3965–3973.
42. McNeill,D.R., Paramasivam,M., Baldwin,J., Huang,J., Vyjayanti,V.N., Seidman,M.M. and Wilson,D.M. 3rd (2013) NEIL1 responds and binds to psoralen-induced DNA interstrand crosslinks. *J. Biol. Chem.*, **288**, 12426–12436.
43. Semlow,D.R., Zhang,J.Q., Budzowska,M., Drohat,A.C. and Walter,J.C. (2016) Replication-dependent unhooking of DNA interstrand cross-links by the NEIL3 glycosylase. *Cell*, **167**, 498.
44. Oparka,M., Walczak,J., Malinska,D., van Oppen,L.M.P.E., Szczepanowska,J., Koopman,W.J.H. and Wieckowski,M.R. (2016) Quantifying ROS levels using CM-H(2)DCFDA and HyPer. *Methods*, **109**, 3–11.
45. Vaisman,A., Varchenko,M., Umar,A., Kunkel,T.A., Risinger,J.I., Barrett,J.C., Hamilton,T.C. and Chaney,S.G. (1998) The role of hMLH1, hMSH3, and hMSH6 defects in cisplatin and oxaliplatin resistance: correlation with replicative bypass of platinum-DNA adducts. *Cancer Res.*, **58**, 3579–3585.
46. Woynarowski,J.M., Faivre,S., Herzig,M.C., Arnett,B., Chapman,W.G., Trevino,A.V., Raymond,E., Chaney,S.G., Vaisman,A., Varchenko,M. *et al.* (2000) Oxaliplatin-induced damage of cellular DNA. *Mol. Pharmacol.*, **58**, 920–927.
47. Furuta,T., Ueda,T., Aune,G., Sarasin,A., Kraemer,K.H. and Pommier,Y. (2002) Transcription-coupled nucleotide excision repair as a determinant of cisplatin sensitivity of human cells. *Cancer Res.*, **62**, 4899–4902.
48. McKay,B.C., Becerril,C. and Ljungman,M. (2001) P53 plays a protective role against UV- and cisplatin-induced apoptosis in transcription-coupled repair proficient fibroblasts. *Oncogene*, **20**, 6805–6808.
49. Corda,Y., Job,C., Anin,M.F., Leng,M. and Job,D. (1991) Transcription by eucaryotic and procaryotic RNA polymerases of DNA modified at a d(GG) or a d(AG) site by the antitumor drug cis-diamminedichloroplatinum(II). *Biochemistry*, **30**, 222–230.
50. Tornaletti,S., Patrick,S.M., Turchi,J.J. and Hanawalt,P.C. (2003) Behavior of T7 RNA polymerase and mammalian RNA polymerase II at site-specific cisplatin adducts in the template DNA. *J. Biol. Chem.*, **278**, 35791–35797.
51. Damsma,G.E., Alt,A., Brueckner,F., Carell,T. and Cramer,P. (2007) Mechanism of transcriptional stalling at cisplatin-damaged DNA. *Nat. Struct. Mol. Biol.*, **14**, 1127–1133.
52. Iyama,T., Lee,S.Y., Berquist,B.R., Gileadi,O., Bohr,V.A., Seidman,M.M., McHugh,P.J. and Wilson,D.M. 3rd (2015) CSB interacts with SNM1A and promotes DNA interstrand crosslink processing. *Nucleic Acids Res.*, **43**, 247–258.
53. Ang,W.H., Myint,M. and Lippard,S.J. (2010) Transcription inhibition by platinum-DNA cross-links in live mammalian cells. *J. Am. Chem. Soc.*, **132**, 7429–7435.
54. Nakano,T., Ouchi,R., Kawazoe,J., Pack,S.P., Makino,K. and Ide,H. (2012) T7 RNA polymerases backed up by covalently trapped proteins catalyze highly error prone transcription. *J. Biol. Chem.*, **287**, 6562–6572.
55. Baker,D.J., Wuenschell,G., Xia,L., Termini,J., Bates,S.E., Riggs,A.D. and O'Connor,T.R. (2007) Nucleotide excision repair eliminates unique DNA-protein cross-links from mammalian cells. *J.Biol. Chem.*, **282**, 22592–22604.
56. Reardon,J.T. and Sancar,A. (2006) Repair of DNA-polypeptide crosslinks by human excision nuclease. *Proc. Natl. Acad. Sci. U.S.A.*, **103**, 4056–4061.
57. Stingele,J., Bellelli,R. and Boulton,S.J. (2017) Mechanisms of DNA-protein crosslink repair. *Nat. Rev. Mol. Cell Biol.*, **18**, 563–573.
58. Horton,J.K., Srivastava,D.K., Zmudzka,B.Z. and Wilson,S.H. (1995) Strategic down-regulation of DNA polymerase beta by antisense RNA sensitizes mammalian cells to specific DNA damaging agents. *Nucleic Acids Res.*, **23**, 3810–3815.
59. Preston,T.J., Henderson,J.T., McCallum,G.P. and Wells,P.G. (2009) Base excision repair of reactive oxygen species-initiated 7,8-dihydro-8-oxo-2′-deoxyguanosine inhibits the cytotoxicity of platinum anticancer drugs. *Mol. Cancer Ther.*, **8**, 2015–2026.

60. Sawant,A., Floyd,A.M., Dangeti,M., Lei,W., Sobol,R.W. and Patrick,S.M. (2017) Differential role of base excision repair proteins in mediating cisplatin cytotoxicity. *DNA Repair (Amst.)*, **51**, 46–59.
61. Wang,D., Xiang,D.B., Yang,X.Q., Chen,L.S., Li,M.X., Zhong,Z.Y. and Zhang,Y.S. (2009) APE1 overexpression is associated with cisplatin resistance in non-small cell lung cancer and targeted inhibition of APE1 enhances the activity of cisplatin in A549 cells. *Lung Cancer*, **66**, 298–304.
62. Yang,J., Parsons,J., Nicolay,N.H., Caporali,S., Harrington,C.F., Singh,R., Finch,D., D'Atri,S., Farmer,P.B., Johnston,P.G. *et al.* (2010) Cells deficient in the base excision repair protein, DNA polymerase beta, are hypersensitive to oxaliplatin chemotherapy. *Oncogene*, **29**, 463–468.
63. Mentegari,E., Kissova,M., Bavagnoli,L., Maga,G. and Crespan,E. (2016) DNA polymerases lambda and beta: the double-edged swords of DNA repair. *Genes (Basel)*, **7**, 57.
64. Martin-Hernandez,K., Rodriguez-Vargas,J.M., Schreiber,V. and Dantzer,F. (2017) Expanding functions of ADP-ribosylation in the maintenance of genome integrity. *Semin. Cell Dev. Biol.*, **63**, 92–101.
65. Audebert,M., Salles,B. and Calsou,P. (2004) Involvement of poly(ADP-ribose) polymerase-1 and XRCC1/DNA ligase III in an alternative route for DNA double-strand breaks rejoining. *J. Biol. Chem.*, **279**, 55117–55126.
66. Boiteux,S., Coste,F. and Castaing,B. (2017) Repair of 8-oxo-7,8-dihydroguanine in prokaryotic and eukaryotic cells: Properties and biological roles of the Fpg and OGG1 DNA N-glycosylases. *Free Radic. Biol. Med.*, **107**, 179–201.
67. Maor-Shoshani,A., Meira,L.B., Yang,X. and Samson,L.D. (2008) 3-Methyladenine DNA glycosylase is important for cellular resistance to psoralen interstrand cross-links. *DNA Repair (Amst.)*, **7**, 1399–1406.
68. Kelley,M.R., Jiang,Y., Guo,C., Reed,A., Meng,H. and Vasko,M.R. (2014) Role of the DNA base excision repair protein, APE1 in cisplatin, oxaliplatin, or carboplatin induced sensory neuropathy. *PLoS One*, **9**, e106485.
69. Dehne,N., Lautermann,J., Petrat,F., Rauen,U. and de Groot,H. (2001) Cisplatin ototoxicity: involvement of iron and enhanced formation of superoxide anion radicals. *Toxicol. Appl. Pharmacol.*, **174**, 27–34.
70. Jiang,Y., Guo,C., Vasko,M.R. and Kelley,M.R. (2008) Implications of apurinic/apyrimidinic endonuclease in reactive oxygen signaling response after cisplatin treatment of dorsal root ganglion neurons. *Cancer Res.*, **68**, 6425–6434.
71. Marullo,R., Werner,E., Degtyareva,N., Moore,B., Altavilla,G., Ramalingam,S.S. and Doetsch,P.W. (2013) Cisplatin induces a mitochondrial-ROS response that contributes to cytotoxicity depending on mitochondrial redox status and bioenergetic functions. *PLoS One*, **8**, e81162.
72. Masuda,H., Tanaka,T. and Takahama,U. (1994) Cisplatin generates superoxide anion by interaction with DNA in a cell-free system. *Biochem. Biophys. Res. Commun.*, **203**, 1175–1180.
73. Brozovic,A., Ambriovic-Ristov,A. and Osmak,M. (2010) The relationship between cisplatin-induced reactive oxygen species, glutathione, and BCL-2 and resistance to cisplatin. *Crit. Rev. Toxicol.*, **40**, 347–359.
74. Kathe,S.D., Shen,G.P. and Wallace,S.S. (2004) Single-stranded breaks in DNA but not oxidative DNA base damages block transcriptional elongation by RNA polymerase II in HeLa cell nuclear extracts. *J. Biol. Chem.*, **279**, 18511–18520.
75. Larsen,E., Kwon,K., Coin,F., Egly,J.M. and Klungland,A. (2004) Transcription activities at 8-oxoG lesions in DNA. *DNA Repair (Amst.)*, **3**, 1457–1468.
76. Kuraoka,I., Endou,M., Yamaguchi,Y., Wada,T., Handa,H. and Tanaka,K. (2003) Effects of endogenous DNA base lesions on transcription elongation by mammalian RNA polymerase II. Implications for transcription-coupled DNA repair and transcriptional mutagenesis. *J. Biol. Chem.*, **278**, 7294–7299.
77. Brooks,P.J. (2008) The 8,5 '-cyclopurine-2 '-deoxynucleosides: Candidate neurodegenerative DNA lesions in xeroderma pigmentosum, and unique probes of transcription and nucleotide excision repair. *DNA Repair*, **7**, 1168–1179.
78. Charlet-Berguerand,N., Feuerhahn,S., Kong,S.E., Ziserman,H., Conaway,J.W., Conaway,R. and Egly,J.M. (2006) RNA polymerase II bypass of oxidative DNA damage is regulated by transcription elongation factors. *EMBO J.*, **25**, 5481–5491.
79. Guo,J., Hanawalt,P.C. and Spivak,G. (2013) Comet-FISH with strand-specific probes reveals transcription-coupled repair of 8-oxoGuanine in human cells. *Nucleic Acids Res.*, **41**, 7700–7712.
80. Kitsera,N., Stathis,D., Luhnsdorf,B., Muller,H., Carell,T., Epe,B. and Khobta,A. (2011) 8-Oxo-7,8-dihydroguanine in DNA does not constitute a barrier to transcription, but is converted into transcription-blocking damage by OGG1. *Nucleic Acids Res.*, **39**, 5926–5934.
81. Menoni,H., Hoeijmakers,J.H. and Vermeulen,W. (2012) Nucleotide excision repair-initiating proteins bind to oxidative DNA lesions in vivo. *The Journal of Cell Biology*, **199**, 1037–1046.
82. Menoni,H., Wienholz,F., Theil,A.F., Janssens,R.C., Lans,H., Campalans,A., Radicella,J.P., Marteijn,J.A. and Vermeulen,W. (2018) The transcription-coupled DNA repair-initiating protein CSB promotes XRCC1 recruitment to oxidative DNA damage. *Nucleic Acids Res.*, doi:10.1093/nar/gky579.
83. Bruno,P.M., Liu,Y., Park,G.Y., Murai,J., Koch,C.E., Eisen,T.J., Pritchard,J.R., Pommier,Y., Lippard,S.J. and Hemann,M.T. (2017) A subset of platinum-containing chemotherapeutic agents kills cells by inducing ribosome biogenesis stress. *Nat. Med.*, **23**, 461–471.
84. Bradsher,J., Auriol,J., Proietti de Santis,L., Iben,S., Vonesch,J.L., Grummt,I. and Egly,J.M. (2002) CSB is a component of RNA pol I transcription. *Mol. Cell*, **10**, 819–829.
85. Koch,S., Garcia Gonzalez,O., Assfalg,R., Schelling,A., Schafer,P., Scharffetter-Kochanek,K. and Iben,S. (2014) Cockayne syndrome protein A is a transcription factor of RNA polymerase I and stimulates ribosomal biogenesis and growth. *Cell Cycle*, **13**, 2029–2037.
86. Pattabiraman,D.R. and Weinberg,R.A. (2014) Tackling the cancer stem cells - what challenges do they pose? *Nat. Rev. Drug Discov.*, **13**, 497–512.
87. Avan,A., Postma,T.J., Ceresa,C., Avan,A., Cavaletti,G., Giovannetti,E. and Peters,G.J. (2015) Platinum-induced neurotoxicity and preventive strategies: past, present, and future. *Oncologist*, **20**, 411–432.
88. Yan,F., Liu,J.J., Ip,V., Jamieson,S.M. and McKeage,M.J. (2015) Role of platinum DNA damage-induced transcriptional inhibition in chemotherapy-induced neuronal atrophy and peripheral neurotoxicity. *J. Neurochem.*, **135**, 1099–1112.
89. McDonald,E.S., Randon,K.R., Knight,A. and Windebank,A.J. (2005) Cisplatin preferentially binds to DNA in dorsal root ganglion neurons in vitro and in vivo: a potential mechanism for neurotoxicity. *Neurobiol. Dis.*, **18**, 305–313.